Maneuvering Multibody Dynamics: New Developments for Models with Fast Solution Scales and Pilot-in-the-Loop Effects

Carlo L. Bottasso, Giorgio Maisano, and Francesco Scorcelletti

Abstract The present paper focuses on trajectory optimization problems for multibody vehicle models, accounting for the presence of pilot-in-the-loop effects and fast dynamic components in the solution. The trajectory optimal control problem is solved through a direct approach by means of a novel hybrid single–multiple shooting method. Specific focus of the present work is the inclusion of pilot models in the optimization process, in order to improve the fidelity of the solution by considering the entire coupled human-vehicle system. In particular we investigate a series of maneuvers flown with helicopters, quantifying the performance loss due to human limitations of the pilot-vehicle system with respect to the sole vehicle case.

1 Introduction

The ability to simulate maneuvers of rotorcraft vehicles flying at the boundaries of their operating envelope is a valuable asset for performance analysis, handling qualities research, design and certification, pilot training, and support to the flight test activity. In general the maneuver of interest can be fully described in terms of quantities which should be minimized of maximized, subject to a variety of equality and inequality constraints [8–13]. Hence, one can usually give a precise mathematical definition of a maneuver by formulating an equivalent optimal control problem. The formulation of such a problem necessitates of a model of the vehicle system with its inputs, states and outputs, of a cost function and of a list of all constraints.

C.L. Bottasso (✉) and G. Maisano
Dipartimento di Ingegneria Aerospaziale, Politecnico di Milano, Via La Masa 34, 20156 Milano, Italy
e-mail: carlo.bottasso@polimi.it; maisano@aero.polimi.it

F. Scorcelletti
Flight Mechanics Department, AgustaWestland, Via Giovanni Agusta 520, 21017 Cascina Costa di Samarate (VA), Italy
e-mail: francesco.scorcelletti@agustawestland.com

K. Arczewski et al. (eds.), *Multibody Dynamics: Computational Methods and Applications*, Computational Methods in Applied Sciences 23,
DOI 10.1007/978-90-481-9971-6_2,

Clearly, the fidelity of the predictions made using this approach crucially hinges on the fidelity of the vehicle model. On the one hand, fidelity improvements may be obtained by considering a more sophisticated description of the vehicle; the current state-of-the-art calls for first-principle multibody models of the vehicle, coupling structural, fluid and servo fields. On the other hand, one might clearly consider the inclusion of a model of the pilot. In fact, in the absence of a pilot model, the solution of a trajectory optimization problem amounts to finding the limit performance trajectory flyable by a "perfect" pilot. In reality, the pilot is a complex system which can be modeled so as to account for sensory perceptions, learned behavior and biomechanical properties. Therefore, it is reasonable to assume that a maneuver optimized considering just a flight mechanics model of the vehicle will in general tend to overestimate the vehicle performance, as this has been computed without accounting for the limitations of various nature of a real pilot. To verify whether this is indeed the case, the present work tries to quantify this hypothesized performance loss due to the inclusion of a pilot model in the trajectory optimization process.

A human pilot model should account for various effects:

- **Sensorial perception**: the sensorial system of the pilot provides for a perception of movements, body position, accelerations, vibrations, etc., which enable the pilot to build a representation of the current situation.
- **Control behavior**: the pilot, based on the input provided by the sensorial information, evaluates the situation and, on the basis of a desired goal, elaborates a control law based on experience and training.
- **Command actuation**: the neuro-musculoskeletal system of the pilot acts like an actuator that takes as input the control law and translates it into movements of the vehicle controls (collective, cyclics, pedal).

In the literature, there is a wide range of pilot models which have been formulated for different applications. As suggested in [21], pilot models can be subdivided in the following categories:

- **Crossover Model**: a basic model for single-axis tracking tasks, which is useful for tuning more complete models. In the region of the open-loop crossover frequency, the product of the pilot transfer function and that of the vehicle is approximated as an integrator with time delay [26].
- **Isomorphic Models**: all models which try to explicitly approximate the dynamics of the human sensory and control systems. The *Structural Model* offers a simplified structural representation of the pilot dynamics in compensatory systems [20, 29]. Particular emphasis is given to sensorial feedback, which typically includes proprioceptive and vestibular feedbacks, while the neuromuscular components of the model is approximated with a second order filter. The *Biophysical Models* give more emphasis to the dynamics of the pilot neuromuscular system [27]. Finally, *Biodynamic Models* are based on multibody dynamics approaches [22], and are used for investigating the effects of an accelerating/vibrating environment on the pilot control capabilities.
- **Algorithmic Models**: models whose principal focus is the control behavior of the pilot, but which may include some isomorphism achieving a good degree of

completeness. A typical example of this category is the *Optimal Control Model*, which considers the human pilot as an optimal controller [17], and where the sensorial component is taken into account by using a Kalman filter.

- **Behavioral Models**: models which consider the human pilot as a black box with nonlinear behavior. There are two principal approaches in this category: *Fuzzy-Logic Models*, which are based on fuzzy-set theory describing cause-and-effect relationships [25, 29], and *Neural Network Models*, which rely upon the capabilities of neural networks of accurately describing nonlinear input-output relationships, mapping pilot cues into control tasks [23].

Clearly, the most appropriate choice of a pilot model is strictly related to the particular application considered. In the framework of trajectory optimization, we need to account for all three aspects listed above, namely sensorial perception, control behavior, and command actuation. Furthermore, it would be preferable to work with a model formulated in state space form, so as to ease its integration in the overall maneuver optimal control problem.

The sensorial perception can be modeled by formulating appropriate observers, for example using Kalman filtering [17]. As a first step towards the goals set forth in this study, we have neglected this aspect of the problem in the present paper, although we plan on considering it in the continuation of this activity. In fact, although the inclusion of an observer in the maneuver optimal control problem formulation does not pose conceptual difficulties, we have postponed the modeling of this component of the pilot system because of the difficulty in finding data for the tuning of the filters.

The second aspect of the modeling, i.e. the control behavior, is in part already included in the formulation of a maneuver optimal control problem. In fact, the pilot elaborates a control law based on desired goals and constraints, which are in fact the very cost function and constraints which enter into the definition of the optimal control problem. However, some aspects of the control behavior are more subtle and difficult to model, such as for example the skills and experience of the pilot. Such effects are hard to model in precise mathematical terms, but we speculate here that they might be rendered through appropriate modifications of the cost function. For example, the modeling of piloting skills might account for degraded piloting behavior for maneuvers which require increased coordination and activity among the controls (increased workload) [15]. Such effects are easily included in the proposed maneuver optimal control approach, since the coding requires trivial modifications to the cost function routines. Nonetheless, specific experimental data are lacking, so that even in this case we have not considered these aspects in the present work, while waiting to perform experiments with pilots in a simulator to gather the observations necessary for the tuning of such models. Therefore, in this paper the control behavior is translated in the choice of a cost function that includes a problem-dependent goal quantity (e.g. altitude loss, time, etc.), and a control term which penalizes excessive control activity and/or excessive control rates; specific details on the choice of the cost functions are given below in the section of the paper devoted to the applications. Such modeling, although rather simple, probably captures a significant, and possibly the most significant, part of the pilot behavior.

The third aspect of the problem, the command actuation, can be modeled in a variety of ways. The more sophisticated approach is based on first-principle modeling of the musculoskeletal system using multibody dynamics, and typically includes rigid bodies with their inertial parameters, joints, muscles with their mechanical and physiological properties, interactional forces with the environment, and other components as required for the accurate representation of the real bio-system. Such level of detail is probably not necessary for capturing the effects of the limitations of the bio-system on the vehicle flight mechanics performance. Hence, a simpler approach is used here, where the effects of the musculoskeletal system are rendered in a global equivalent sense through the use of simple delay and filter models, as detailed below.

There are two principal approaches to the solution of trajectory optimization problem: indirect [16, 28] and direct methods [5–7, 10, 13]. Following our previous work [11], we prefer the direct approach even for the applications which are the focus of the present paper. In fact, in the case of the indirect methods one has first to derive the optimal control governing equations by using the calculus of variation, and then numerically solve the arising two-point boundary value problem. The manipulation of the vehicle equations of motion for deriving the optimal control governing equations makes it very hard or inefficient, if not altogether impossible, to use black-box flight simulators, where more often than not one does not have access to the source code. In the case of coupled vehicle-pilot models, the equations tend to become even more involved, so that here again the use of a direct approach allows for a simpler implementation. In fact, the direct approach does not require any manipulation of the equations, as one first discretizes the problem by time stepping (using either a transcription or a shooting method [11]) and then solves the resulting Non-Linear Programming (NLP) problem by a standard solver, such as SQP (Sequential Quadratic Programming).

Multibody vehicle models of rotorcraft systems include both slow flight mechanics scales and faster aero-elastic ones [14]. To treat more effectively this class of optimal control problems of multibody systems, we use multiple shooting on the flight mechanics scales, and single shooting on the faster aero-elastic ones; this avoids the enforcement of the multiple shooting gluing constraints for the faster scales, which greatly enhances convergence and in turn reduces the computational cost.

The paper is organized according to the following plan. At first, we describe the pilot model considered in this work and we present the equations of the coupled pilot-vehicle system. Secondly, we formulate in general terms the trajectory optimization problem. A discussion about the possible numerical solution strategies to solve this problem are given next; namely, we first describe the direct transcription approach and then we present the direct hybrid single–multiple shooting method. Finally, we investigate a number of maneuvering rotorcraft problems, and we assess the pilot-in-the-loop effects on the computed limit performance of the vehicle.

2 Coupled Pilot-Vehicle Model

As argued in the introduction, enriching a vehicle model by adding a pilot model is a way to improve the performance predictions made using trajectory optimization. The main task of a pilot is to govern the vehicle by deciding a suitable control law in relation with the maneuver goals, based on the current perception of the situation as provided by his/her sensory system. The optimal control model proposed in [24] and revisited in [17] is a possible way of rendering these effects. In the present work we adopt a similar approach, reformulating it in the context of trajectory optimization. This way, the decision level control behavior of the pilot can be considered as embedded in the objective function of the maneuver optimal control problem.

The two remaining aspects of human pilot limitations are due to sensorial perceptions and command actuation. As a first step towards the more ambitious goal of a complete pilot modeling system, we consider here a simple actuator pilot model (Fig. 1), in order to assess its impact on the vehicle performance predictions, as well as on the computational cost and robustness of the numerical procedures.

The vehicle equations of motion can be expressed as

$$\boldsymbol{f}(\dot{\boldsymbol{x}}, \boldsymbol{x}, \boldsymbol{u}, t) = 0, \tag{1}$$

where $\boldsymbol{x}$ are the flight mechanics states, and $\boldsymbol{u}$ the vehicle control inputs (collective, longitudinal and lateral cyclics, and pedal). More in general, rotorcraft multibody models are described in terms of differential–algebraic equations which also include Lagrange multipliers and constraint equations; however, in the sole interest of a lighter notation and simpler discussion, we consider in the following the ordinary differential set of equations expressed by (1).

The pilot actuator system is modeled using a pure time delay [17], operating in series with a second order filter for the neuromuscular element [29] for each control input. The pure time delay is approximated by a second-order Padè transfer function, which provides excellent accuracy over the frequency range of the pilot (0.1–10 rad/s) [17]; for the single channel we have:

$$Y_d(s) = \frac{1 - \frac{1}{2}(\tau s) + \frac{1}{8}(\tau s)^2}{1 + \frac{1}{2}(\tau s) + \frac{1}{8}(\tau s)^2}. \tag{2}$$

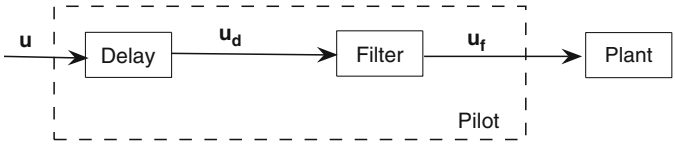

Fig. 1 Pilot model: pure delay and second-order filter

The second-order filter [29] is written as

$$Y_f(s) = \frac{\omega_{NM}^2 s}{s^2 + 2\zeta_{NM}\omega_{NM} s + \omega_{NM}^2}. \tag{3}$$

The series of delay and filter on each control channel can be written in linear state space form as

$$\dot{\boldsymbol{x}}_p = \boldsymbol{A}\,\boldsymbol{x}_p + \boldsymbol{B}\,\boldsymbol{u}, \tag{4a}$$
$$\boldsymbol{u}_f = \boldsymbol{C}\,\boldsymbol{x}_p + \boldsymbol{D}\,\boldsymbol{u}, \tag{4b}$$

where $\boldsymbol{x}_p$ is the neuromuscular state of length $4n_u$, where the number of control inputs n_u is equal to 4 for a rotorcraft vehicle. The elements of matrices $\boldsymbol{A}$, $\boldsymbol{B}$, $\boldsymbol{C}$ and $\boldsymbol{D}$ depend on the delay and filter parameters, and in particular on the time constant τ of the pure delay, and on the damping factor ζ_{NM} and undamped natural frequency ω_{NM} of the open-loop neuromuscular system. Referring to Fig. 1, it should be noted that the inputs of the pure time delay module are the "desired" command pilot inputs $\boldsymbol{u}$, while the inputs of the neuromuscular module are the delayed command inputs $\boldsymbol{u}_d$. Finally, the delayed and filtered inputs $\boldsymbol{u}_f$ actuate the rotorcraft vehicle model.

Collecting together (1) and (4), we can write the governing equations of the coupled pilot-vehicle model as

$$\dot{\boldsymbol{x}}_p = \boldsymbol{A}\,\boldsymbol{x}_p + \boldsymbol{B}\,\boldsymbol{u}, \tag{5a}$$
$$\boldsymbol{u}_f = \boldsymbol{C}\,\boldsymbol{x}_p + \boldsymbol{D}\,\boldsymbol{u}, \tag{5b}$$
$$\boldsymbol{f}(\dot{\boldsymbol{x}}, \boldsymbol{x}, \boldsymbol{u}_f, t) = 0. \tag{5c}$$

Formally, by collecting all states in a unique state vector $\boldsymbol{x}_{\mathrm{pv}}^T = (\boldsymbol{x}^T, \boldsymbol{x}_p^T)^T$, by collecting all dynamic equations (5) into a single function $\boldsymbol{f}_{\mathrm{pv}}$ and eliminating all algebraic equations, we can write the governing equations of the coupled pilot-vehicle system in the following compact form:

$$\boldsymbol{f}_{\mathrm{pv}}(\dot{\boldsymbol{x}}_{\mathrm{pv}}, \boldsymbol{x}_{\mathrm{pv}}, \boldsymbol{u}, t) = 0. \tag{6}$$

When optimizing a maneuver considering only the stand-alone vehicle model, one uses (1); on the other hand, when the pilot is included in the optimization the augmented system (6) is used. Formally, the two are identical, so that no changes are necessary to the trajectory optimization software for dealing with the coupled pilot-vehicle model.

3 Formulation of Maneuvers as Optimal Control Problems

A maneuver can be defined as a dynamic transition between two steady state (trimmed) configurations [18], although in the present context it is useful to give a looser interpretation of the term by considering also the case of terminal conditions

which are not trimmed. Clearly, given a starting and arrival configuration, there is an infinite number of ways to transition between the two. A possible way to remove this arbitrariness is to formulate a maneuver as a constrained optimal control problem [8–10, 13].

The maneuver optimal control problem requires the minimization or maximization of a cost or merit function (e.g. time, altitude loss, control activity, fuel consumption, etc.), which in general can be expressed in terms of the vehicle states or outputs and of the control inputs. Furthermore, the optimization problem is constrained by a number of conditions that should be met by the solution:

- First, the so-called compatibility conditions must be fulfilled at each time instant of the maneuver; in other words, it is required that the computed solution satisfies the equations of motion of a suitable flight mechanics model of the vehicle.
- Second, the solution should remain within the flight envelope and operational limits of the vehicle.
- Finally, most maneuvers of practical interest (Category-A, ADS-33, flare at the exit of an autorotation, etc.) are typically characterized by other equality and inequality constraints which need to be met in order to satisfy given performance and procedural requirements and that, collectively, contribute to giving a precise definition of the maneuver of interest.

The maneuver optimal control problem can be formally expressed as:

$$\min_{\boldsymbol{x},\boldsymbol{y},\boldsymbol{u},T} \quad J = \phi(\boldsymbol{y},t)\big|_0^T + \int_0^T L(\boldsymbol{y},\boldsymbol{u},\dot{\boldsymbol{u}},t)\,\mathrm{d}t, \tag{7a}$$

$$\text{s.t.:} \quad \boldsymbol{f}(\dot{\boldsymbol{x}},\boldsymbol{x},\boldsymbol{u}) = 0, \tag{7b}$$

$$\boldsymbol{y} = \boldsymbol{h}(\boldsymbol{x},\boldsymbol{u}), \tag{7c}$$

$$\boldsymbol{g}(\boldsymbol{y},\boldsymbol{u},t) \in [\boldsymbol{g}^{\min},\boldsymbol{g}^{\max}]. \tag{7d}$$

Solving the problem consists in finding the control function $\boldsymbol{u}(t)$, and hence through (7b) and (7c) the associated functions $\boldsymbol{x}(t)$ and $\boldsymbol{y}(t)$, which minimize the cost J given by (7a). In general, the cost includes a boundary quantity which accounts for values of the outputs at the initial and/or final instants, as well as an integral cost term. The problem is defined on the interval $\Omega = [0, T]$, $t \in \Omega$, where the final time T is typically unknown and must be determined as part of the solution to the problem.

The model governing equations appear among the problem constraint conditions, and are expressed by (7b) and (7c), where $\boldsymbol{x}$ are the states, $\boldsymbol{u}$ the inputs and $\boldsymbol{y}$ the outputs. As shown in the previous section, the model governing equations (7b) can be represented by (1) when considering the stand-alone vehicle model, or by (6) for the coupled pilot-vehicle case.

All maneuver-defining and/or envelope-protection constraints are expressed as generic algebraic non-linear constraints by (7d). These may include as special cases boundary (initial ($t = 0$) and/or terminal ($t = T$)) conditions, constraints at

unknown internal time events ($t = T_i$), generic constraints defined over the whole maneuver duration ($t \in [0, T]$), which clearly may also include, as it is often the case in practical applications, simple bounds on the inputs and states/outputs.

4 Direct Solution of Maneuver Optimal Control Problems

As discussed in [11], the direct approach is often the preferable way to solve the optimal control problem (7), for a series of practical advantages with respect to the classical indirect method. According to the direct approach, the optimal control problem is first discretized and subsequently optimized. This procedure yields a discrete parameter optimization or NLP problem [19], which can be written as

$$\min_{z} \quad K(z), \tag{8a}$$

$$\text{s.t.} \quad \boldsymbol{a}(z) = \boldsymbol{0}, \tag{8b}$$

$$\boldsymbol{b}(z) \in [\boldsymbol{b}^{\min}, \boldsymbol{b}^{\max}], \tag{8c}$$

where z is a vector of algebraic unknowns, and K is a scalar objective function which represents an approximation of the cost J of (7a). The equality constraints (8b) are generated by the discretization of the equations of motion (7b,7c), while the inequality constraints (8c) by all other maneuver-defining constraints (7d). Notice that the problem defined by (8) is characterized by unknown algebraic parameters z, while the optimal control problem (7) by functional unknowns.

The specific form of the vector of algebraic unknowns and of the constraints in problem (8) depends on the method used for performing the discretization. Our software program `TOP` (Trajectory Optimization Program) [11] implements both the direct transcription and the direct multiple shooting methods, which are briefly reviewed next.

4.1 Direct Transcription

This method is very effective and robust, but it is typically applicable only to models which have low-moderate complexity [13], i.e. which do not have solution time scales which are too fast with respect to the overall maneuver duration, and/or do not possess too large a number of states.

The time interval Ω is partitioned as $0 = t_0 < t_1 < \cdots < t_N = T$, where the generic time element is $\Omega^n = [t_n, t_{n+1}]$, $n = (0, N-1)$, of time step size $h^n = t_{n+1} - t_n$. On each time element Ω^n, the governing equations (7b) are discretized using a suitable numerical method. The resulting discrete equations are expressed as

$$\boldsymbol{f}_h(\boldsymbol{x}_{n+1}, \boldsymbol{x}_n, \boldsymbol{u}^n, h^n) = 0, \qquad n = (0, N-1), \tag{9}$$

where $\boldsymbol{f}_h$ is an algorithmic approximation of function $\boldsymbol{f}$ of (7b), $\boldsymbol{x}_n$, $\boldsymbol{x}_{n+1}$ are the values of the state vector at t_n and t_{n+1}, respectively, while $\boldsymbol{u}^n$ represents the value of the control vector within the step. In general there might be additional internal stages for both the state and the control variables, depending on the numerical method [11].

The NLP problem (8) is defined as follows. First, the NLP vector of parameters is chosen as:

$$z = (\boldsymbol{x}_{n=(0,N)}, \boldsymbol{u}^{n=(0,N-1)}, T)^T, \tag{10}$$

i.e. it is defined by the discrete states and control values on the computational grid, and the final time. Notice that, if one needs a very large number of time steps to accurately resolve the solution, the size of z will be large, up to the point of making this approach unsuitable in terms of computational burden.

Next, the cost J of (7a) is discretized in terms of z as given by (10), obtaining the discrete cost K of (8a). Then, the discretized ODEs within each step, (9), become the set of NLP equality constraints appearing in (8b). Finally, all other problem constraints and bounds, (7d), are expressed in terms of the NLP variables z and become the NLP inequality constraints of (8b).

4.2 Direct Multiple and Hybrid Single–Multiple Shooting

Multiple shooting is typically used in applications of moderate/high complexity, i.e. with solution time scales which are fast with respect to the maneuver duration, and/or a moderate/large number of degrees of freedom [13].

The time domain Ω is partitioned as $0 = t_0 < t_1 < \cdots < t_M = T$ with $\Omega^m = [t_m, t_{m+1}]$, $m = (0, M-1)$, where each Ω^m is a shooting segment. In each shooting segment Ω^m, the controls are discretized as $\boldsymbol{u}^m(t) = \sum_{i=1}^{N_c^m} s_i(t)\boldsymbol{u}_i^m$, where $s_i(t)$ are basis functions, in particular cubic splines in the present implementation, and $\boldsymbol{u}_i^m$ are N_c^m unknown discrete control values. The control approximations are confined on each shooting segment; this has the effect of decreasing the computational cost of finite differencing by increasing the problem sparsity. Constraints are enforced at the shooting segment boundaries to guarantee the continuity of the controls up to C^1.

In the case of direct multiple shooting, the NLP problem (8) is defined as follows. First, the NLP unknown parameters are chosen as:

$$z = \left(\boldsymbol{x}_{m=(0,M)}, \boldsymbol{u}_{i=(1,N_c^m)}^{m=(0,M-1)}, T\right)^T, \tag{11}$$

i.e. they represent the discrete values of the states at the interfaces between shooting segments, the discrete values of the controls within each segment, and the final time.

Next, the governing ODEs (7b) are marched in time within each shooting segment Ω^m, starting from the initial conditions provided by the values of the states $\boldsymbol{x}_m$ at the left boundary of the segment. The effect of the forward integration is to generate a discrete time history of states within Ω^m, which we label $\boldsymbol{x}_i^m$, $i = (1, N^m)$, where N^m is the number of steps taken in that segment. The last value of this

sequence is named $\widetilde{\boldsymbol{x}}_{m+1} = \boldsymbol{x}^m_{N^m}$, and represents the new estimate of the state variables at the right boundary of the shooting segment. Segments are then glued together by imposing the following equality constraints

$$\boldsymbol{x}_m - \widetilde{\boldsymbol{x}}_m = 0, \qquad m = (2, M). \tag{12}$$

Multiple shooting segments are used for stabilizing the forward integration of the vehicle equations of motion [4]. This is particularly important when analyzing unstable systems, which is often the case when considering rotorcraft vehicles.

Notice that the size of the unknown parameter vector $\boldsymbol{z}$ is unrelated to the time step size used for marching the equations of motion within shooting arcs; hence, one may use very fine temporal discretizations without impacting the overall problem size, which in fact enables the solution of problems with a higher degree of complexity than in the direct transcription case [13].

In the direct multiple shooting case, the cost J of (7a) is discretized in terms of $\boldsymbol{z}$ as given by (11) and evaluated using the segment time histories $\boldsymbol{x}^m_i$; this yields the discrete cost K of (8a). Next, the gluing conditions (12) are used to express the set of NLP equality constraints appearing in (8b). All other problem constraints and bounds, (7d), are expressed in terms of the NLP variables $\boldsymbol{z}$ and become the NLP inequality constraints of (8b).

For complex multibody systems denoted both by slow and fast solution components, we have observed that the satisfaction of the multiple shooting gluing constraints can be particularly difficult and usually ends up dominating the problem. Once again a rotorcraft multibody model provides for an excellent illustration of such difficulties. In fact, models have flight mechanics states which describe the gross rigid body motion of the vehicle through the position, orientation, linear and angular velocities of a body-attached (or floating, in the case of a flexible fuselage) frame of reference, as well as fast scales which are typically related to the rotor degrees of freedom, and include rigid and flexible blade states and aerodynamic states.

Often, a naive implementation of multiple shooting fails to achieve convergence for such complex multi-scale models. This is not surprising, since the rotor generates most of the aerodynamic forces acting on the vehicle and even small variations in its states may imply large variations in the resulting forces, which hinders the satisfaction of the gluing constraints.

We have found that these problems can be alleviated by using multi-time scale arguments [14]. In fact, the rotor states (both structural and aerodynamic) are significantly faster than the flight mechanics ones. Thus, since the multiple shooting treatment of these fast states is the main cause of the two aforementioned issues, i.e. raise in computational cost and difficulty in satisfying gluing constraints, one can think of treating slow and fast scales using different methods.

More specifically, a multiple shooting approach is used for the slow states. This is crucial, since with single shooting small changes early in the trajectory can produce dramatic effects at the end of it [4]; clearly, the problem is exacerbated when analyzing unstable systems. Hence, the multiple shooting treatment of slow scales avoids the blow up of the solution.

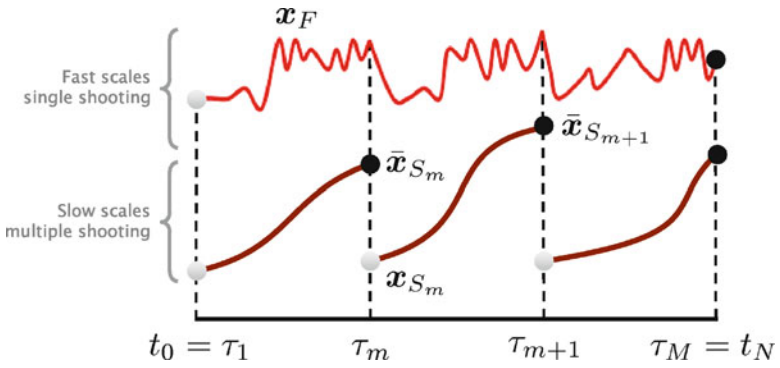

Fig. 2 Hybrid single–multiple shooting approach

On the contrary, fast scales are treated using a single shooting approach, as depicted in Fig. 2. This does not compromise the robustness of the procedure, since fast scales will not diverge if slow ones do not; hence, the stabilizing effect produced by the multiple shooting treatment of slow scales is felt also at the level of the fast ones.

With such a hybrid single–multiple shooting approach, the size of the resulting NLP problem is substantially reduced and so is the total computational cost. Furthermore, there are no gluing constraints to be enforced for the fast rotor states, since only the slow states need to be glued together at the shooting interfaces. This has the effect of greatly increasing the robustness of the procedure, and the convergence speed.

5 Applications and Results

In this section we consider the solution of maneuver optimal control problems of practical interest. We analyze the ADS-33 Lateral Reposition Mission Task Element (MTE) [3] for handling qualities assessment, as well as a Category-A fly-away [2]. Goal of these two examples is a first preliminary assessment of the effects of the inclusion of the simplified pilot model described earlier on in this work with respect to the computed limit performance.

The helicopter model, implemented using the rotorcraft multibody `FLIGHTLAB` code [1], represents a generic medium-size multi-engine four-bladed utility vehicle in the 9 ton class.

5.1 Lateral Reposition MTE

The ADS-33E-PRF specification [3] for military rotorcraft defines a series of MTEs which provide a basis for an overall assessment of the vehicle ability to perform

certain critical tasks, and result in an assigned level of handling qualities according to the Cooper–Harper rating scale. Each MTE is related to a maneuver that shall be accomplished considering specific constraints, as described in [3]. In fact, it is possible to formulate each MTE as a constrained optimal control problem [12]. Hence, with a software implementation of the procedures discussed in this work, it is possible to readily compile a library of MTEs of interest in order to predict the handling qualities characteristics of a specific rotorcraft.

We analyze here the Lateral Reposition MTE, considering both the stand-alone vehicle model and the coupled pilot-vehicle system.

According to the Lateral Reposition MTE [3], the helicopter, initially in hover, is supposed to translate laterally for 400 ft and then recover the initial hover configuration. The maneuver must be flown in ground effect since the initial and final positions are characterized by an altitude of 35 ft (the rotor diameter is 30 ft); altitude variations must be within ± 10 ft. Referring to Fig. 3, the maximum allowed displacement in the longitudinal direction is ± 10 ft, while the maximum heading misalignment is ± 10 deg with respect to the initial direction. The maneuver must be completed within 18 s.

One possible formulation of this MTE is to consider the following minimum time cost function (13):

$$J = T + \frac{1}{T} \int_0^T \dot{\boldsymbol{u}} \cdot \boldsymbol{W} \dot{\boldsymbol{u}} \, \mathrm{d}t. \tag{13}$$

The first term enforces the minimum time condition, while $\boldsymbol{W} = \mathrm{diag}(\boldsymbol{w}_{\dot{u}})$ is a diagonal matrix of tunable weighting factors which penalize the control rates.

It is also necessary to constrain the vehicle trajectory so as to express the MTE path requirements described above. With this formulation of the problem the time constraint is not explicitly enforced, but verified a posteriori. In other words, one tunes the weight parameters $\boldsymbol{W}$ in the merit function (13), this way controlling the aggressiveness of the maneuver. Then, once a solution has been computed, one verifies whether the maneuver was rapid enough and effectively completed within the maximum allotted time. Obviously there are limitations in the maneuver aggressiveness related to the vehicle capabilities and its flight envelope constraints. In this case the trajectory constraints are imposed directly through bounds on the position variables and heading angle:

$$|\psi(t)| \leq 10 \,\mathrm{deg}, \tag{14a}$$

$$|x(t)| \leq 10 \,\mathrm{ft}, \tag{14b}$$

$$|\Delta z(t)| \leq 10 \,\mathrm{ft}, \tag{14c}$$

$$0 \leq y(t) \leq 400 \,\mathrm{ft}. \tag{14d}$$

We solved this problem initially without considering a pilot model; once the "pilot-off" solution had been evaluated, we used it as the initial guess for the evaluation of the "pilot-on" case. The following values for the pilot actuator model were used [29]: $\tau = 0.2$ s, $\omega_{NM} = 10$ rad/s, $\zeta_{NM} = \cos(\pi/4)$.

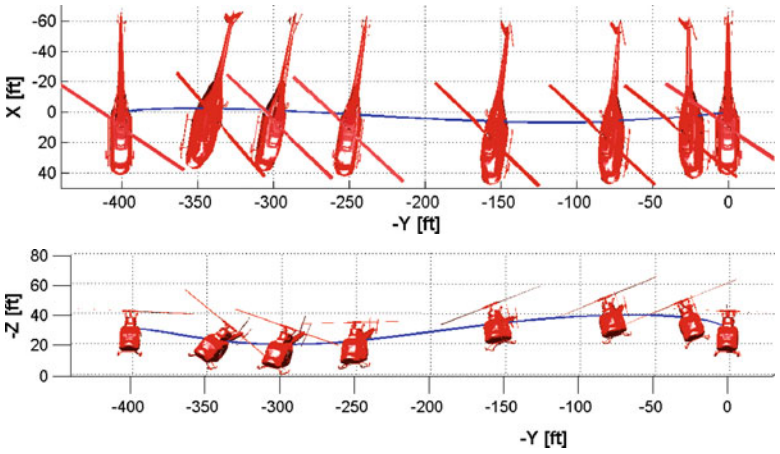

Fig. 3 Lateral Reposition MTE: snapshots

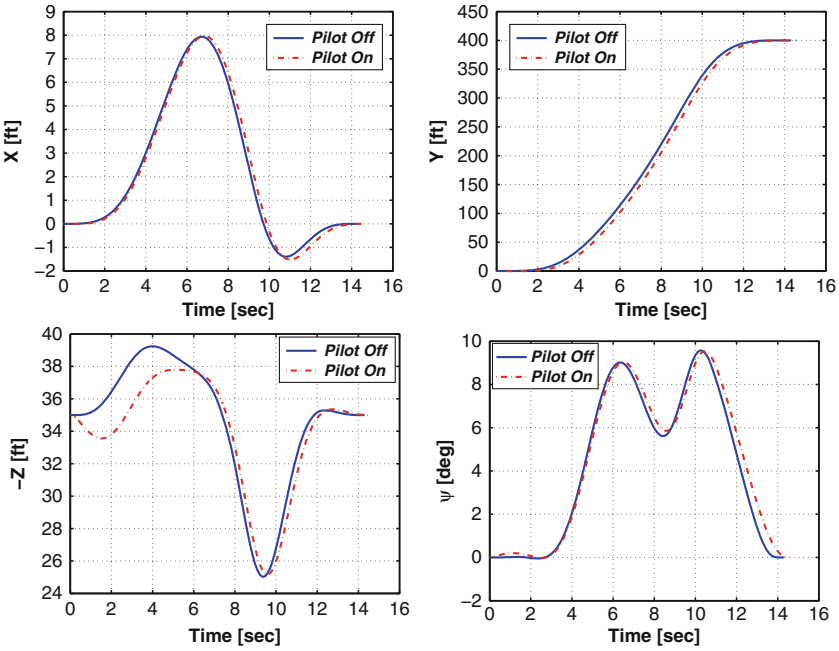

Fig. 4 Lateral Reposition MTE: X, Y, Z positions, and heading angle (from *top* to *bottom*, *left* to *right*)

Figure 3 shows some snapshots of the helicopter during the maneuver. Figure 4 gives the time histories of the constrained path variables, for both the pilot-off (solid lines) and the pilot-on cases (dash-dotted lines). Figure 5 shows the control time history; in the pilot-on case, both the computed pilot model inputs (vector $\boldsymbol{u}$ in (5)) and the plant inputs (vector $\boldsymbol{u}_f$ in (5)) are shown in the figure.

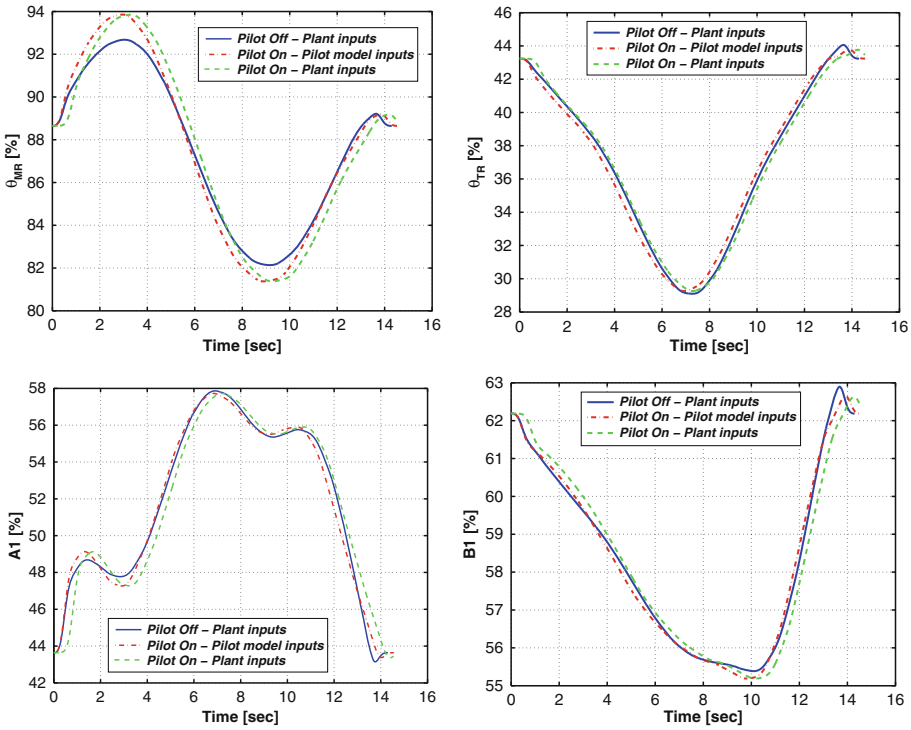

Fig. 5 Lateral Reposition MTE: collective, pedal, lateral and longitudinal cyclic (from *top* to *bottom*, *left* to *right*)

The pilot-in-the-loop effects do not appear to generate significant differences with respect to the stand-alone vehicle model for both the trajectory and the control inputs. The maneuver duration is in both cases less than the 18 s prescribed by the normative, with a slightly longer total time for the pilot-on case. Both trajectory and controls do not not appear to have been significantly affected by the neuromuscular lag.

5.2 Category-A Fly-Away

The effect of pilot actuation are investigated also for the case of a fly-away maneuver under Category A certification requirements [2]. A meaningful simulation policy for such a maneuver consists in the minimization of the altitude loss, according to the cost

$$J = H(T) + \frac{1}{T}\int_0^T \dot{\boldsymbol{u}} \cdot \boldsymbol{W}\dot{\boldsymbol{u}}\,\mathrm{d}t, \tag{15}$$

The initial condition is a hover. A latency period of 1.2 s after the engine failure is taken into account, during which the pilot realizes the situation and there is no control activity. The power loss is modeled as

$$P_{av}(t) = P_H + (P_{OEI} - P_H)\, K^+(t) + P_H\, K^-(t), \tag{16a}$$

$$K^+(t) = \mathrm{sca}(t - t_0)(1 - e^{-t/\tau^+}), \tag{16b}$$

$$K^-(t) = \mathrm{sca}(t - t_0)e^{-(t-t_0)/\tau^-}, \tag{16c}$$

where t_0 is the instant of engine failure, P_H is the hover power, $P_{OEI} = 1750$ HP is the one engine inoperative maximum take-off power available, while $\tau^+ = 2/9$ s and $\tau^- = 1/9$ s are suitable time constants. An inequality constraint in the maneuver optimal control problem (7d) is used for ensuring that the power generated by the engine is at all times less than the available one, as expressed by (16a). The final conditions are

$$W(T_f) = 0 \text{ m/s}, \tag{17a}$$

$$p(T_f) = q(T_f) = r(T_f) = 0 \text{ deg/s}, \tag{17b}$$

$$\Omega(T_f) \geq 90\%. \tag{17c}$$

All simulations were conducted outside of ground effect. This single-phase formulation of the problem considers only the first part of the maneuver, i.e. from the engine loss to the moment the lowest point in the trajectory is reached. A multi-phase formulation of the same problem covering also the climb part of the Category-A maneuver was considered in [8–10].

The standard procedure is to fly this emergency maneuver in the longitudinal plane of the helicopter. In fact, simulations of this maneuver are often conducted with a two-dimensional helicopter model. However, using a three-dimensional model, one may observe that the solution converges to a three-dimensional maneuver with significant yaw and roll (see Fig. 6). The three-dimensional (3D) optimal maneuver altitude loss $\Delta H^{3D}_{\min} = 15.77$ m improves on the two-dimensional (2D)

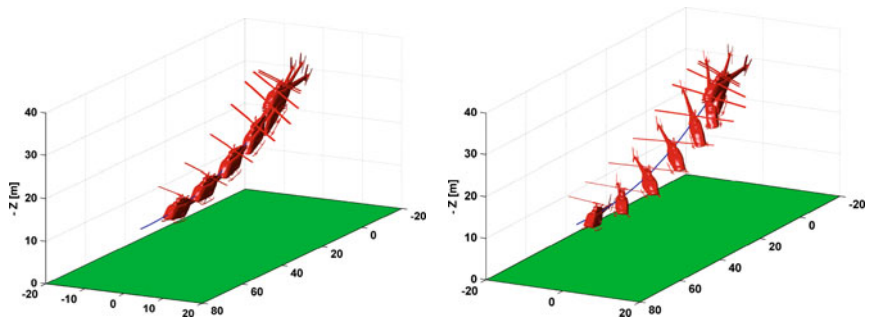

Fig. 6 Category A, fly-away: optimal two-dimensional (*left*) and three-dimensional (*right*) trajectories, pilot-off case

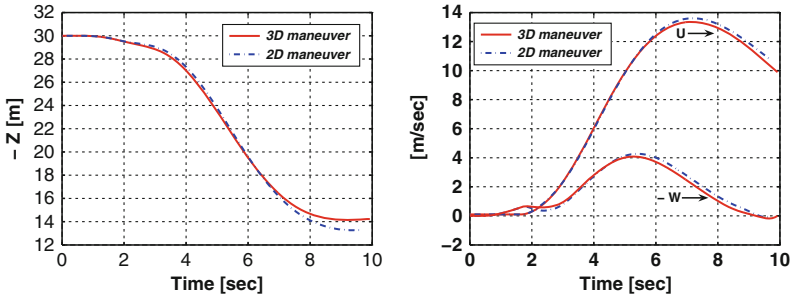

Fig. 7 Category A, fly-away: altitude loss comparison (*left*) and inertial velocities (*right*), pilot-off case

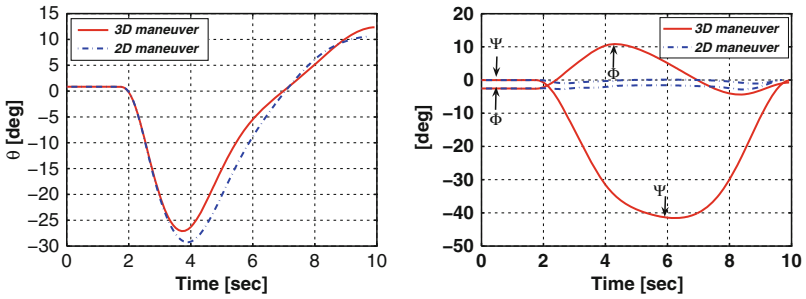

Fig. 8 Category A, fly-away: helicopter attitude, pilot-off case

optimal altitude loss $\Delta H^{2D}_{min} = 16.72\,m$ of about one meter (Fig. 7 at *left*), as confirmed by the opinion of test pilots. This gain can be explained by observing Fig. 8. In the 3D maneuver, both the roll and yaw angles increase and reach their respective maxima approximatively halfway throughout the maneuver. This attitude allows for some reduction in the vertical velocity (Fig. 7 at *right*), which explains the decreased altitude loss. Clearly, the control activity on the pedal and lateral cyclic is higher for the 3D maneuver than for the 2D one.

These two simulations were repeated including the pilot model. To simplify convergence, we used a bootstrapping procedure. The first guess was initialized to the solution computed without pilot model. Next, the control time histories of the guess solution were used for evaluating the pilot model dynamic constraints, thus obtaining initial estimates of the pilot state time histories. The stand-alone vehicle solution augmented with the pilot state time histories was then used as initial guess for the pilot-in-the-loop optimization.

For the coupled pilot-vehicle problem, the resulting optimal maneuvers do not change significantly in terms of control input profiles with respect to pilot-off simulations, but the altitude loss increases for both the 2D and 3D cases (see Fig. 9). In the 2D maneuver the altitude loss is $\Delta \hat{H}^{2D}_{min} = 18.56\,m$ with a difference of 1.84 m (10.38 %) with respect to the pilot-off case, while in the 3D case we obtain $\Delta \hat{H}^{3D}_{min} = 17.62\,m$ with a difference of 1.85 m (11.73 %). This is not simply due to

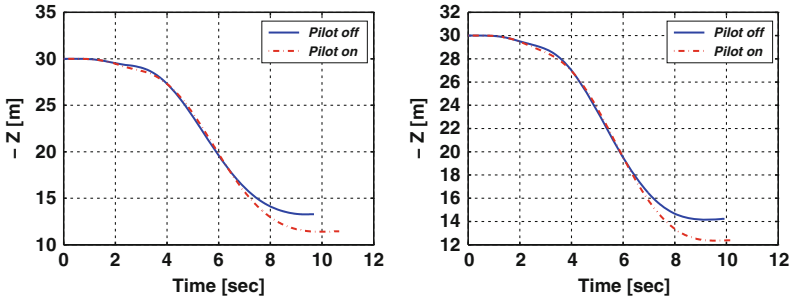

Fig. 9 Category A maneuver, fly-away: altitude loss comparison (*left*: 2D; *right*: 3D)

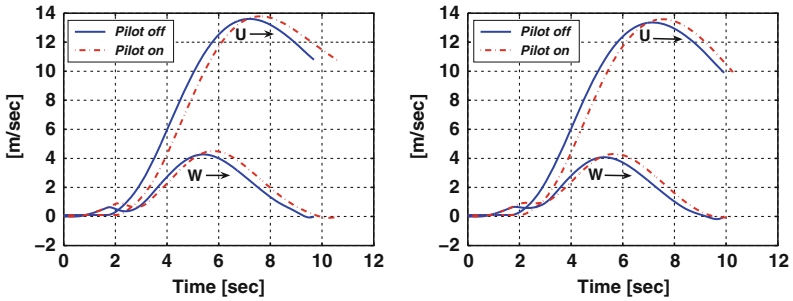

Fig. 10 Category A maneuver, fly-away: inertial velocities (*left*: 2D; *right*: 3D)

the fact that all time histories are delayed. The principal reason appears to be the delay in the pilot first reaction to the engine loss, which gives a higher maximum vertical velocity value, as shown in Fig. 10.

In conclusion, the introduction of a pilot model seems to have a non negligible effect on the performance estimation, which would seem to motivate further refinements in the simplified pilot model considered in this preliminary study. Furthermore, it appears that a 3D maneuver gives better performance (less altitude loss), than the usual 2D one. However, the 3D maneuver is harder to fly since it requires good coordination skills. Moreover, the pronounced sideslipping might make it difficult for the pilot to hold the visual references.

6 Concluding Remarks

In this work we have formulated a trajectory optimization approach to maneuver modeling in rotorcraft flight mechanics, including pilot-in-the-loop effects and fast dynamic solution components.

The formulation can accommodate the pilot control behavior as part of the definition of the cost function (and in this sense falls within the category of optimal control pilot models), as well as the command actuation and sensorial perception

aspects. In this work, the command actuation was rendered using global equivalent models through the use of a simple delay in series with a second order filter. Although a more sophisticated model, as for example a biomechanical multibody model, could be readily implemented in the formulation without conceptual difficulties, the present implementation is probably sufficient for capturing the relevant command actuation effects on the flight mechanics characteristics of the response. The sensorial perception component of the model was not considered here, mainly for the lack of sufficiently reliable data for the tuning of the required Kalman-based observers; this aspect of the problem is currently under investigation, and will be reported in a forthcoming publication. It is reasonable to speculate that the inclusion of the perception system model will determine further degradation of the performance, although the actual quantification of this aspect remains to be seen.

Based on the current state of this study, the following conclusions may be drawn:

- The performance degradation due to pilot-in-the-loop effects depends on the particular maneuver considered. In particular, it appears that for the Lateral Reposition MTE the pilot model induces negligible differences, while the Category-A rejected take-off shows a more pronounced effect with an increased altitude loss. Other maneuvers will be considered in the continuation of the present study.
- The inclusion of a pilot model in the optimal control formulation does not imply substantial difficulties, since the coupled pilot-vehicle system is formally identical to a generic vehicle model expressed in non-linear state space form.
- The current version of the pilot model has only a modest impact on the computational cost of the optimization, so that the code retains its ability to conduct complete maneuver simulations in the order of minutes on standard desktop computers.
- As for all optimization problems, better performance and robustness of the procedures relies also on good initial guesses of the solution, which in this case also requires initial estimates of the internal pilot states. This was achieved here using a bootstrapping procedure, based on an initial solution computed without pilot model, followed by the initialization of the pilot states obtained with the computed pilot-off control inputs. This procedure proved to be easy to implement and very effective.

Acknowledgements The present research is supported by AgustaWestland through a grant with the Politecnico di Milano, Marco Cicalè being the main project monitor. Simulations using the `FLIGHTLAB` code were conducted at the AgustaWestland headquarters in Cascina Costa, Italy, using AgustaWestland licenses. The contribution of C. Ravaioli and A. Ragazzi in the preparation of the examples is gratefully acknowledged.

References

1. Advanced Rotorcraft Technology, Inc., 1685 Plymouth Street, Suite 250, Mountain View, CA 94043. http://www.flightlab.com
2. Anonymous (1999) Advisory circular 29-2C, certification of transport category rotorcraft. Federal Aviation Administration, Department of Transportation

3. Anonymous (2000) Handling qualities requirements for military rotorcraft. Aeronautical Design Standard, U.S. Army Aviation and Missile Command, Aviation Engineering Directorate, Rept. ADS-33E-PRF, Redstone Arsenal, AL
4. Ascher UM, Mattheij RMM, Russell RD (1995) Numerical solution of boundary value problems for ordinary differential equations. Classics in Applied Mathematics, SIAM, vol 13, Philadelphia
5. Betts JT (2001) Practical methods for optimal control using non-linear programming. SIAM, Philadelphia
6. Betts JT (1998) Survey of numerical methods for trajectory optimization. J Guid Cont Dynam 21(2):193–207
7. Bottasso CL, Croce A (2004) Optimal control of multibody systems using an energy preserving direct transcription method. Multibody Syst Dyn 12:17–45
8. Bottasso CL, Croce A, Leonello D, Riviello L (2005) Optimization of critical trajectories for rotorcraft vehicles. J Am Helicopter Soc 50:165–177
9. Bottasso CL, Croce A, Leonello D, Riviello L (2005) Rotorcraft trajectory optimization with realizability considerations. J Aerospace Eng 18:146–155
10. Bottasso CL, Chang C-S, Croce A, Leonello D, Riviello L (2006) Adaptive planning and tracking of trajectories for the simulation of maneuvers with multibody models. Comput Meth Appl Mech Eng 195:7052–7072
11. Bottasso CL, Maisano G, Scorcelletti F (2008) Trajectory optimization procedures for rotorcraft vehicles, their software implementation and applicability to models of varying complexity. American Helicopter Society 64th Annual Forum, Montréal, Canada. Also: J Am Helicopter Soc, under review
12. Bottasso CL, Scorcelletti F, Maisano G, Cicalè M, Ragazzi A (2008) Mission task elements and critical maneuvers simulation for rotorcraft vehicles. Rotorcraft Handling Qualities Conference, University of Liverpool, Liverpool, UK
13. Bottasso CL (ed.) (2008) Solution procedures for maneuvering multibody dynamics problems for vehicle models of varying complexity. Multibody dynamics – computational methods and applications, Computational Methods in Applied Sciences, ISBN 978-1-4020-8828-5, Springer, Dordrecht, The Netherlands
14. Bottasso CL, Maisano G (2009) Efficient rotorcraft trajectory optimization using comprehensive vehicle models by improved shooting methods. 35th European Rotorcraft Forum, Hamburg, Germany
15. Bradley R, MacDonald CA, Buggy TW (2005) Quantification and prediction of pilot workload in the helicopter/ship dynamic interface. J Aerospace Eng 219(5):29–443
16. Bryson AE, Ho YC (1975) Applied optimal control. Wiley, New York
17. Davidson JB, Schmidt DK (1992) Modified optimal control pilot model for computer-aided design and analysis. NASA, TM 4348, NASA Langley Research Center, Hampton, VA, USA
18. Frazzoli E (2001) Robust hybrid control for autonomous vehicle motion planning. Ph.D. Thesis, Department of Aeronautics and Astronautics. Massachusetts Institute of Technology, Cambridge, MA, USA
19. Gill PE, Murray W, Wright MH (1981) Practical optimization. Academic Press, London and New York
20. Hess RA (1997) Unified theory for aircraft handling qualities. J Guid Control Dynam 20(6):1141–1148
21. Hess RA (2006) Simplified technique for modelling piloted rotorcraft operations near ships. J Guid Control Dynam 29(6):1339–1349
22. Höhne G (2000) Computer aided development of biomechanical pilot models. Aero Sci Tech 4:57–69
23. Jagacinski RJ (2003) Control theory for humans – Quantitative approaches to modeling performance. Erlbaum, Mahwah, NJ
24. Kleinman DL, Baron S, Levison WH (1970) An optimal control model of human response. Part I: theory and validation. Part II: prediction of human performance in a complex task. Automatica 6:357–38

25. Kramer U (1985) On the application of fuzzy sets to the analysis of the system-driver-vehicle environment. Automatica 3(1):101–107
26. McRuer DT, Krendel ES (1974) Mathematical models of human pilot behavior. NATO AGAR-Dograph No. 188, Paris, France
27. Van Paassen R (1994) Biophysics in aircraft control: a model of the neuromuscular system of the pilot's arm. Ph.D. Thesis, Faculty of Aerospace Engineering. Delft University of Technology, The Netherlands
28. Veeraklaew T, Agrawal SK (2001) New computational framework for trajectory optimization of higher-order dynamic systems. J Guid Control Dynam 24(2):228–236
29. Zeyada Y, Hess RA (2000) Modelling human pilot cue utilization with application to simulator fidelity assessment. J Aircraft 37(4):558–597

http://www.springer.com/978-90-481-9970-9

Multibody Dynamics
Computational Methods and Applications
Arczewski, K.; Blajer, W.; Fraczek, J.; Wojtyra, M. (Eds.)
2011, VIII, 327 p., Hardcover
ISBN: 978-90-481-9970-9